Astronomy & Astrophysics

Dust in starburst nuclei and ULIRGs

SED models for observers

R. Siebenmorgen[1] and E. Krügel[2]

[1] European Southern Observatory, Karl-Schwarzschildstr. 2, 85748 Garching b. München, Germany
e-mail: `rsiebenm@eso.org`
[2] Max-Planck-Institut für Radioastronomie, Auf dem Hügel 69, Postfach 2024, 53010 Bonn, Germany

ABSTRACT

Aims. We provide a library of some 7000 SEDs for the nuclei of starburst and ultra luminous galaxies. Its purpose is to quickly obtain estimates of the basic parameters, such as luminosity, size and dust or gas mass and to predict the flux at yet unobserved wavelengths. The procedure is simple and consists of finding an element in the library that matches the observations. The objects may be in the local universe or at high z.

Methods. We calculate the radiative transfer in spherical symmetry for a stellar cluster permeated by an interstellar medium with standard (Milky Way) dust properties. The cluster contains two stellar populations: old bulge stars and OB stars. Because the latter are young, a certain fraction of them will be embedded in compact clouds which constitute hot spots that determine the MIR fluxes.

Results. We present SEDs for a broad range of luminosities, sizes and obscurations. We argue that the assumption of spherical symmetry and the neglect of clumpiness of the medium are not severe shortcomings for computing the dust emission. The validity of the approach is demonstrated by matching the SED of seven of the best studied galaxies, including M 82 and Arp 220, by library elements. In all cases, one finds an element which fits the observed SED very well, and the parameters defining the element are in full accord with what is known about the galaxy from detailed studies. We also compare our method of computing SEDs with other techniques described in the literature.

Key words. infrared: galaxies – galaxies: starburst – Galaxy: nucleus

1. Introduction

By definition, the rapid conversion of a large amount of gas into predominantly massive (>8 $M_\odot$) stars, or the result of such a conversion, is called a starburst. Starburst galaxies constitute a unique class of extragalactic objects. The phenomenon is of fundamental importance to the state and evolution of the universe, as outlined, for example, in the review by Heckman (1998). According to him, in the local universe ($z < 0.1$) starbursts are responsible for about 25% of the high-mass star formation rate and for 10% of the total luminosity; in the early universe, beyond $z \sim 0.7$, IR luminous galaxies dominate the star forming activity (Floc'h et al. 2005). Starbursts are also cosmologically significant if one interprets the high bolometric luminosities of high redshift galaxies to be due to star formation (Chary & Elbaz 2001; Hirashita et al. 2003) at a rate so high that it can only be maintained over a cosmologically short spell (<10^8 yr). The study of nearby starbursts would then help us to understand the processes underlying the star formation history of the universe.

Starbursts, we think, are triggered by the gravitational interaction between galaxies (Kennicutt et al. 1987), but they occur, as a result of mass and angular momentum transfer, predominantly in their nuclei, at the center of a massive and dynamically relaxed cluster of old stars (the bulge). Although the region where OB stars form is relatively small (a few hundred parsec), its luminosity often exceeds that of the host galaxy. Starbursts are almost pure infrared objects, opaque to stellar photons. Whereas, on average, in the local universe ~60% of the star formation is obscured by dust (Takeuchi et al. 2006), in starbursts the fraction is typically 90%. To interpret infrared observations and to arrive at a self-consistent picture for the spatial distribution of stars and interstellar matter in the starburst nucleus and of the range of dust temperatures, one has to simulate the transfer of continuum radiation in a dusty medium. Line emission is energetically negligible.

A starburst has four basic parameters: total luminosity, L, dust or gas mass, M_d or M_{gas}, visual extinction, A_V, and size. Size, A_V and M_d are, of course, related, for a homogeneous density model, only two of them are independent. The luminosity follows observationally in a straight forward way by integrating the spectral energy distribution over frequency, M_d is readily derived from a millimeter continuum data point, if available, and the outcome is almost independent of the internal structure or viewing angle of the starburst. The size is best obtained from radio observations as it does not suffer extinction by dust. It does not matter whether the radio emission is thermal or non-thermal, both are connected to high-mass stars.

In this paper, we present a set of spectral energy distributions (SEDs) for starbursts covering a wide range of parameters. Anyone with infrared data and interested in their interpretation can compare them with our models, find an SED that matches (after normalization of the distance) and thus constrain the properties of the starburst under investigation without having to perform a radiative transfer computation himself.

2. Dust model and radiative transfer

A description of the dust model and the radiative transfer can be found in chapter 12 and 13 of Krügel (2003), we here only summarize the salient points. We use standard dust. It consists of silicate and amorphous carbon grains with a size distribution ($n(a) \propto a^{-3.5}$, $a \sim 300 \dots 2400$ Å), and a population of small graphite grains ($a \sim 10 \dots 100$ Å). There are also two kinds of polycyclic aromatic hydrocarbons (PAH) ($N_C = 38, N_H = 12$ and $N_C = 250, N_H = 48$, where N_C, N_H are the number of C, H atoms, respectively). By mass, 63% of the dust is in silicates, 37% in carbon of which 60% is amorphous, 38% graphitic and 2% in PAHs. About 5% of the graphitic particles are so small (<60 Å) that their temperature fluctuates. Such a dust mixture produces reddening in rough agreement with the standard interstellar extinction curve for $R_V = 3.1$.

An important feature of our model is the division of the sources in the starburst nucleus into two classes.

a) OB stars in dense clouds with total luminosity L_{OB}. The immediate surroundings of such a star constitutes a hot spot and its emission must be evaluated separately as they, more than anything else, determine the mid infrared (MIR) part of the SED of a galactic nucleus (Krügel & Tutokov 1978; Krügel & Siebenmorgen 1994). The outer radius of a hot spot, R_{hs} is given by the condition of equal heating of the dust from the star and from the ambient radiation field. The hot spots, whose total volume is small compared to the volume of the galactic nucleus, are presented in the radiative transfer equation by a continuously distributed source term $\varepsilon_\nu^{hs}(r)$, where r is the distance towards the center of the galactic radius. For a fixed OB stellar luminosity, ε_ν^{hs} is sensitive to the assumed density in the hot spot, ρ^{hs}.

b) The total luminosity of all other stars is $L_{tot} - L_{OB}$. These are mainly the old bulge stars of low brightness and surface temperature, but also hotter stars not enveloped in a dense cloud. This population is presented in the radiative transfer equation by a continuously distributed source term $\varepsilon_\nu^{bulge}(r)$.

The model galactic nucleus is a sphere (of radius R) and the radiative transfer is computed with ray tracing. The intensity, $I_\nu(p, z)$, is a function of frequency ν, impact parameter p, and coordinate z. At different ν and p, we solve along the z-axis the equations

$$I^+(\tau) = I^+(0)\, e^{-\tau} + \int_0^\tau S(x)\, e^{x-\tau}\, dx \qquad (1)$$

$$I^-(t) = \int_0^t S(x)\, e^{x-t}\, dx \qquad (2)$$

I^+ and I^- refer to the plus and minus direction of z, respectively. The indices p and ν have been omitted. The optical depth τ is zero at $z = 0$ and increases with z, the optical depth t is zero at the edge of the nucleus (where $z_e = \sqrt{R^2 - p^2}$) and decreases with z. There is no radiation incident from outside, so $I^-(z = z_e) = I^-(t = 0) = 0$, and symmetry requires $I^+ = I^-$ at $z = 0$. The source function (dropping sums over different kinds of dust particles) equals

$$S_\nu = \frac{1}{K_\nu^{ext}} \cdot \left[\varepsilon_\nu^{hs} + \varepsilon_\nu^{bulge} + K_\nu^{sca} J_\nu + K_\nu^{abs} \int P(T) B_\nu(T)\, dT \right]. \qquad (3)$$

The term $K_\nu^{abs} \int P(T) B_\nu(T)$ describes the emission of dust grains. If they are big, the probability density $P(T)$ equals the δ-function $\delta(T_d)$ where T_d follows from the equilibrium between radiative heating and cooling. For small grains, $P(T)$ is evaluated

in an iterative scheme similar to the method of Guhathakurta & Draine (1989). J_ν is the galactic radiation field. As we assume isotropic scattering, we reduce the Mie scattering efficiency, Q^{sca}, by the factor $(1 - g_\nu)$, where g_ν is the asymmetry factor. All quantities depend on the galactic radius, r. The emission from the hot spots is calculated separately in a radiative transfer program for an OB star in a spherical cloud of density ρ^{hs} bathed in the radiation field of the galactic nucleus.

3. Parameter space of the model grid

For our set of SEDs, we vary in the calculations the following five parameters:

1. total luminosity L^{tot} from 10^{10} to 10^{14} $L_\odot$ in steps of 0.1 in the exponent;
2. nuclear radius, $R = 0.35$, 1 and 3 kpc;
3. the visual extinction from the edge to the center of the nucleus: $A_V \simeq 2.2, 4.5, 7, 9, 18, 35, 70$ and 120 mag;
4. ratio of the luminosity of OB stars with hot spots to the total luminosity: $L_{OB}/L^{tot} = 0.4, 0.6$ and 0.9;
5. dust density in the hot spots. For a gas-to-dust ratio of 150, the corresponding hydrogen number densities are $n^{hs} = 10^2, 10^3$ and 10^4 cm^{-3}. The density is constant within the hot spot.

Not all parameter combinations are included in the set of SEDs because some are astronomically unlikely (for instance, very high L^{tot} and very little extinction). Altogether, the grid contains 7000 entries.

The dust density in the nucleus, ρ, is spatially constant, $\partial\rho/\partial r = 0$. Its value follows from the extinction A_V and the nuclear radius, R. The dust mass, M_d, is then given by $4\pi\rho R^3/3$ and increases linearly with A_V. For example, for $R = 350$ pc and $A_V = 18$ mag, the gas mass, M_{gas}, is 1.7×10^8 $M_\odot$. The density of all stars is centrally peaked, $\rho_*(r) \propto r^{-1.5}$.

The OB stars are always confined to the inner 350 pc, and they have a fixed luminosity and surface temperature (2×10^4 $L_\odot$, $T_{eff} = 25\,000$ K). The bulge stars fill the total volume. As they do not form hot spots, we need not specify the luminosity of a single star. For $L_{tot} \leq 10^{12.7}$ $L_\odot$, their surface temperature, T_{eff}, equals 4000 K (old giants). When $L_{tot} > 10^{12.7}$ $L_\odot$, we assume $T_{eff} = 25\,000$ K, which means that they consist mainly of OB stars, but outside compact clouds.

Figure 1 illustrates the changes in the SED when one parameter is varied while all others stay fixed; fluxes refer to a source distance of 50 Mpc. Panel a informs us how a rise in luminosity shifts the far IR peak to shorter wavelengths. The flux then increases in the near IR much more strongly than at submillimeter wavelengths. If $L_{tot} \geq 10^{12.5}$ $L_\odot$, the large grains become so warm that at $\lambda > 11$ μm they outshine the PAH features. In panel b, we see that as the source becomes bigger, the dust gets cooler (maximum emission at longer wavelengths). This is not because the dust is then, on average, farther away from the source, but because the dust mass, M_d, grows with R^2 when A_V is constant, and the mean dust temperature is determined by L^{tot}/M_d. We also see that a high ratio of L_{OB}/L^{tot} enhances the near IR flux. Panel c shows the influence of the density in the hot spots for $n^{hs} = 10^2, 10^3$ and 10^4 cm^{-3}, it is particular strong in the MIR. Panel d depicts the influence of the optical depth. Large values suppress the near IR emission and produce absorption in the 10 μm, and for very high extinctions ($A_V \geq 70$ mag) also in the 18 μm silicate bands.
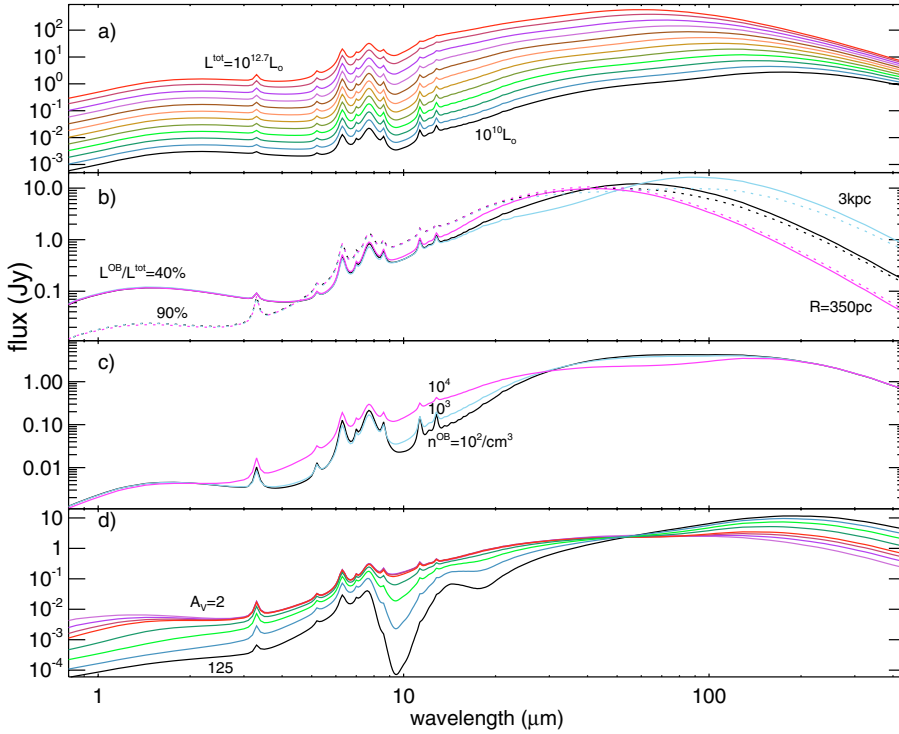
Fig. 1. Influence of starburst parameters on the SED for a distance of 50 Mpc. The parameters which are kept constant are listed in square parentheses. **a)** Total luminosity is varied between $L^{tot} = 10^{10}$ and $10^{12.7}\,L_\odot$; [$R = 3$ kpc, $A_V \sim 17$ mag, $L_{OB}/L^{tot} = 0.6$ and $n^{hs} = 10^3$ cm^{-3}]. **b)** Here we vary two parameters: the radius of the nucleus from $R = 0.35$ over 1 to 3 kpc, and the luminosity ratio: $L_{OB}/L^{tot} = 0.4$ (full lines), 0.9 (dotted); [$L^{tot} = 10^{11.1}\,L_\odot$, $A_V \sim 4.5$ mag and $n^{hs} = 10^4$ cm^{-3}]. **c)** Variation of the hot spot density: $n^{hs} = 10^2$, 10^3 and 10^4 cm^{-3}; [$L^{tot} = 10^{10.5}\,L_\odot$, $R = 3$ kpc, $A_V \sim 9$ mag, $L_{OB}/L^{tot} = 0.9$]. **d)** Variation of the dust extinction: $A_V \sim 2.2$, 4.5, 6.7, 9, 18, 35, 70 and 125 mag; [$L^{tot} = 10^{10.5}\,L_\odot$, $R = 3$ kpc, $L_{OB}/L^{tot} = 0.9$ and $n^{hs} = 10^4$ cm^{-3}].

4. Testing the SED library

4.1. Fitting prototypical galaxies

We put our library of ~7000 theoretical SEDs to the test by applying it to seven famous and well studied galaxies of the local universe, five starbursts (M 82, NGC 253, NGC 7714, NGC 1808, NGC 7552) and two ULIRGs (NGC 6240 and Arp 220). The observational data and our fits are displayed in Figs. 2 to 5, underlying model parameters are listed in Table 1. The seven galaxies, discussed in more detail below, cover a wide range of luminosities and we check:

– whether their observed spectra can be reasonably matched or, at least, bracketed by elements of the set;
– whether there is only one matching element or, at most, a few which are similar in their basic parameters;
– whether the parameters of the matching element are meaningful, i.e. whether they are consistent with the information about the structure of the galactic nucleus which we already have.

M 82

The present model for this archetype starburst is similar to the one proposed before (Krügel & Siebenmorgen 1994). The latter was shown only for $\lambda \geq 3\,\mu$m. At shorter wavelengths, the observed flux does not steeply decline, as the old model predicts and as one would expect judging from the silicate feature (its depth implies $A_V \geq 15$ mag). Therefore, either hard radiation leaks out because of clumps or funnels created by supernova explosions, or there are stars in M 82 outside the opaque nuclear dust clouds. As our model cannot handle clumping, but we nevertheless wish to extend the spectrum into the UV, we simply add another stellar component. It is not included in a self-consistent way, but as its luminosity is ~10% of the total, such an approximation may be tolerable. The stellar temperature and foreground reddening of the additional component are poorly constrained (see caption of Fig. 2). This is also reflected by the controversial

interpretations via an old stellar population (Silva et al. 1998) or via young, but obscured stars (Efstathiou et al. 2000).

We mention that Sturm et al. (2000) contest the existence of the 10 μm silicate absorption feature in M 82. They think that the value $\tau(18\,\mu\text{m})\,/\,\tau(9.7\,\mu\text{m})$ is too low and that recombination line ratios, like H_β/H_α, indicate only $A_V \simeq 5$. However, the small ratio $\tau(18\,\mu\text{m})/\tau(9.7\,\mu\text{m})$ is a radiative transfer effect where 18 μm emission is favored over 10 μm emission, and the H_β/H_α ratio increases when the dust is not a foreground screen, as Sturm et al. assume, but mixed with the HII gas. The strongest argument that the 10 μm depression is due to silicates comes from the 1 mm flux. It implies a large column density of cold dust which, unless it is all behind the hot dust, must produce the absorption feature.

NGC 253

NGC 253, another bright and nearby starburst, shows at high resolution in the MIR a complex structure with several knots (Galliano et al. 2005). Nevertheless, the low spatial resolution observations are well reproduced in our fit (Fig. 3) which, in the 10−40 μm wavelength range, is of similar quality as in M 82 (Fig. 2). Below 2 Jy, ISOSWS data are noisy and have therefore been omitted. The dip at 18 μm in the model of Piovan et al. (2006) is not present in ours, and not borne out by the observations. As our model dust is uncoated, the ice features reported by Imanishi et al. (2003) are not reproduced.

NGC 7714

Spitzer spectra (Brandl et al. 2004) do not reveal signatures of an active galactic nuclei (AGN) and support our interpretation that the nucleus is dominated by a weakly obscured starburst (Fig. 3).

NGC 1808

This starburst is claimed to be young (Krabbe et al. 1994). In high resolution MIR images, several hot spots are detected
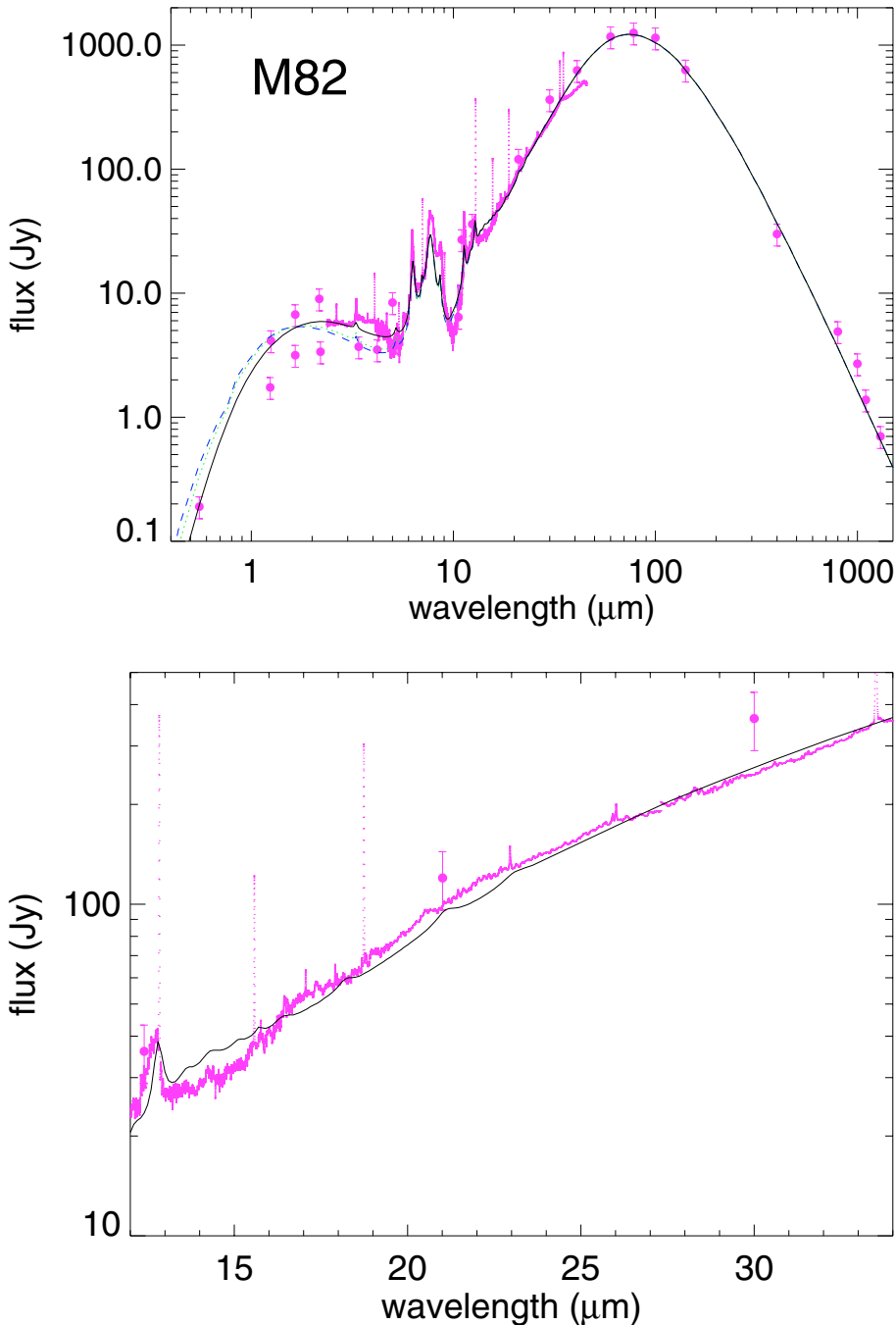
Fig. 2. SED of the central region of M 82, data points with 1σ error bar. Full line: library model with parameters in Table 1. To fit the data below 5 μm, we added to the SED library spectrum a blackbody, either unreddened ($T = 2500$ K, full line), or reddened ($T = 8000$ K, $A_V = 4$ mag, dashed, or $T = 5000$ K, $A_V = 3$ mag, dotted). *Top*: full wavelength range from 0.4 to 1500 μm, *bottom*: a zoom into the 12−34 μm region. Data references (1300 μm: Krügel et al. 1990; 1100 and 800 μm: Hughes et al. 1990; 400 μm: Jaffee et al. 1984; far IR: Telesco & Harper 1980; Rieke & Low 1972; Rieke et al. 1980; Telesco & Gezari 1992; IRAS; near infrared (NIR) photometry in 40″−100″ aperture: Kleinmann & Low 1970; Jarrett et al. 2003; Aaronson 1977; and Johnson 1966; between 2.3–40.4 μm ISOSWS spectrum: Sloan et al. 2003).

which coincide with the most intense radio sources (Galliano et al. 2005). Our fit (Fig. 4) somewhat underestimates the PAH emission. So one may have to increase the PAH abundance (as was done in the model of Siebenmorgen et al. 2001) which is set constant in the computations of our SED library. Piovan et al. (2006) predict silicate absorption features at 10 and 18 μm which, however, are not detected. The dip at ~10 μm is due to the wings of neighboring PAH bands. It is not caused by silicate self-absorption which would require much higher optical depths.

NGC 7552

This infrared luminous galaxy harbors a ring-like circumnuclear starburst (Siebenmorgen et al. 2004). Neglecting such structural details, our fit to the dust emission is satisfactory. Two models

are shown in Fig. 4 which bracket available data. The hot spot density is low and the OB luminosity ratio, L_{OB}/L_{tot}, is not well constrained (Table 1).

NGC 6240

NGC 6240 is a merging ULIRG. Such objects are one to two orders of magnitude brighter than starbursts. Our fit in Fig. 5 is acceptable despite a ~30% deficiency near 40–50 μm. To better match the NIR photometry, we added to the starburst SED a 4000 K black body with $L = 10^{8.8}\ L_\odot$. Lutz et al. (2003) suggest that stars account for most (~75%) of the total luminosity and that the rest is due to an optically obscured AGN. When they subtract from the SED of NGC 6240 a scaled-up M 82 template, a faint (0.07 Jy) residue remains which they

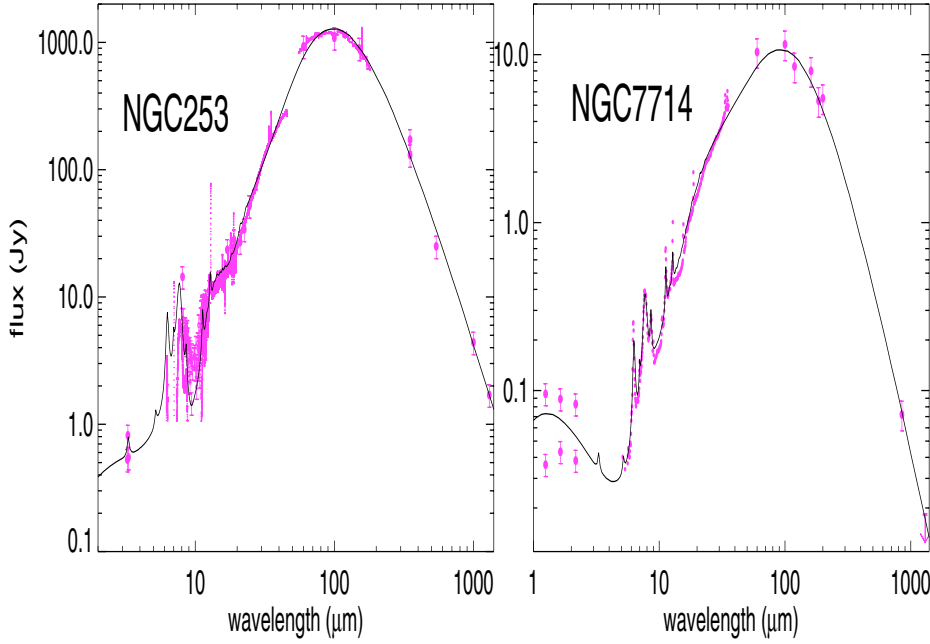**Fig. 3.** SEDs of NGC 253 and NGC 7714, data points with 1σ error bar. Models: full lines, model parameters in Table 1. Data for NGC 253 (ISOSWS: Sloan et al. 2003; ISOLWS and ISOPHT: Radovich et al. 2001; NIR: Rieke & Low 1975; IRAS; submm: Rieke et al. 1973; Hildebrand et al. 1977; Chini et al. 1984). Data for NGC 7714 (NIR in 40″–100″ aperture: Spinoglio et al. 1995; Jarrett et al. 2003; Spitzer IRS: Brandl et al. 2004; IRAS; ISOPHT: Krügel et al. 1998; 850 μm: Dune et al. 2000; 1.3 mm: Krügel et al. 1998).
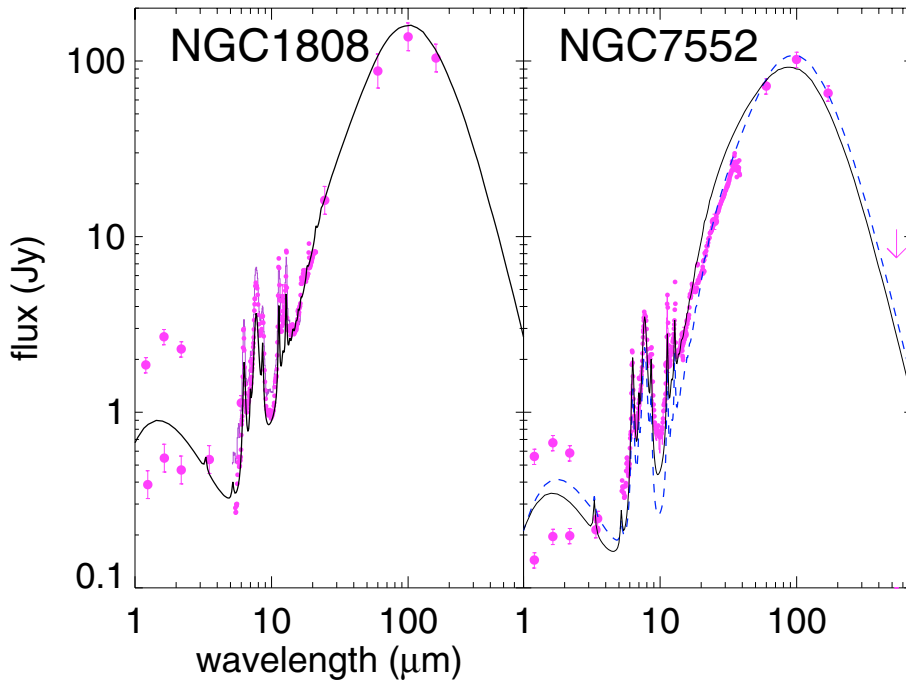

Fig. 4. SEDs of NGC 1808 and NGC 7552, data points with 1σ error bar. Models: full and dashed lines, model parameters in Table 1. Data for NGC 1808 (NIR in 40″–100″ aperture: Glass 1976; Jarrett et al. 2003; IRAS; ISOPHT 160 μm and ISOCAM spectroscopy: Siebenmorgen et al. 2001). Data for NGC 7552 (NIR in 40″–100″ aperture: Glass 1976; Jarrett et al. 2003; ISOCAM: Roussel et al. 2001; TIMMI2: Siebenmorgen et al. 2004; Spitzer IRS of nucleus: Kennicutt et al. 2003; IRAS; submm: Stickel et al. 2004; Hildebrand et al. 1977).

attribute to the AGN. Dopita et al. (2005) underestimate in their model the 10–30 μm region (by a factor ~4 at 15 μm) but they argue that they could match the data if they added an AGN component, a procedure which is sometimes applied to galaxies with hidden broad line regions (Efstathiou & Siebenmorgen 2005).

Arp 220

Arp 220 is the nearest example of a ULIRG. MIR high resolution maps (Soifer et al. 2002) show a double nucleus with 1″ (360 pc) separation. We process low resolution Spitzer IRS data using the Spitzer pipeline (Higdon et al. 2004). The ISOPHT (Spoon et al. 2004) and Spitzer spectrum reveals a complex spectrum with ice and silicate absorption and pronounced PAH emission bands at 6.2 and 7.7 μm. Dopita's et al. (2005) model predicts

PAH features that are too strong (factor >5). Piovan et al. (2006) fit the SED of the central 2 kpc region using an optical depth of $\tau_V = 35$ mag and a dust model with an SMC extinction curve. Siebenmorgen et al. (1999) proposed $\tau_V = 54$ mag and MW dust to fit the photometric data available at that time. The SED library fit gives $R = 3$ kpc and $A_V = 72$ mag. A model SED with $A_V = 120$ mag and $R = 1$ kpc yields too strong silicate absorption and requires an additional cold dust component for the submm.

4.2. Luminosity and flux prediction

The infrared luminosity is the key parameter of a galaxy and it is often used to estimate the star formation rate of a galaxy (Kennicut 1998). Unfortunately, for faint or redshifted objects
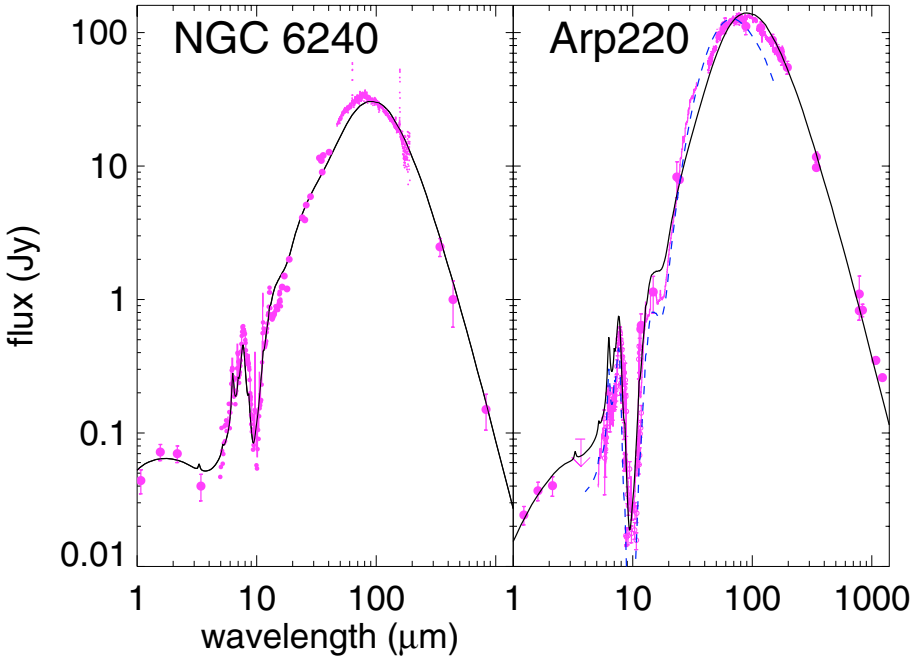
Fig. 5. SEDs of NGC 6240 and Arp 220, data points with 1σ error bar. Models: full and dashed lines, model parameters in Table 1. To match *JHK* photometry of NGC 6240, we added a 4000 K black body to the starburst model. Data for NGC 6240 (NIR: Spinoglio et al. 1995; ISOPHT and submm: Klaas et al. 1997, 2001; 350 μm: Benford 1999; ISOCAM spectroscopy: Laurent et al. 2000; ISOPHT and ISOSWS: Lutz et al. 2003). Data for Arp 220 (2MASS: Jarrett et al. 2003; IRAS; ISOPHT: Klaas et al. 2001; ISOCAM: Siebenmorgen & Efstathiou 2001; submm: Benford 1999; Rigopoulou 1996; Dunne et al. 2000; Carico et al. 1992; Chini et al. 1986; ISOLWS archive spectrum is scaled to match the ISOPHT photometry and Spitzer IRS spectrum (this work)).

Table 1. Fit parameters to models of Figs. 2–5.

Name	L^{tot} $L_\odot$	D Mpc	R kpc	A_V mag	L_{OB}/L^{tot}	n^{hs} cm^{-3}
M 82	$10^{10.5}$	3.5	0.35	36	0.4	10^4
NGC 253	$10^{10.1}$	2.5	0.35	72	0.4	7500
NGC 7714	$10^{10.7}$	36.9	3	2	0.6	2500
NGC 1808	$10^{10.7}$	11.1	3	5	0.4	1000
NGC 7552	$10^{11.1}$	22.3	3	7	0.6	100
"	"	"	"	9	0.4	"
NGC 6240	$10^{11.9}$	106	3	36	0.6	10^4
Arp 220	$10^{12.1}$	73	1	120	0.4	10^4
"	"	"	3	72	"	"

Table 2. The number of models in the library which fit observations of NGC 6240 at the indicated wavelengths to better than 30%. Columns 3 and 4 give their range in luminosity and reddening.

observed wavelengths (μm)	No. of models	$\log L^{tot}$ $L_\odot$	A_V
8, 16	26	11.4–12.3	2–144
8, 25	36	11.6–12.1	2–72
16, 25	9	11.6–12.1	2–72
8, 16, 25	9	11.6–12.1	18–72
8, 70	8	11.8–12.1	18–144
25, 70	6	11.8–11.9	18–144
16, 70	4	11.8–12.1	36–144
8, 16, 70	4	11.8–12.2	36–144
8, 25, 70	4	11.8–11.9	18–72
16, 25, 70	2	11.8–11.9	36–72

photometry is sometimes only provided at two MIR bands, for example at 8 and 24 μm from the Spitzer satellite.

To determine the scatter in the expected source luminosity when only two or three infrared points are available, we select from the model library all objects which agree with the measured points to within 30%. This corresponds to assuming a photometric uncertainty of 30%. The resulting range in the model luminosity and in the obscuration A_V is shown in Table 2.

A 70 μm and a MIR point constrain L^{tot} already very well, which is no surprise as all galaxies peak in the far infrared. With a second MIR point, one can also confine A_V within a reasonable range. On the other hand, two broad band data in the mid IR alone, where the instrumental sensitive is higher, yield hardly any information on the obscuration, but limit L^{tot} within a factor of three. Three MIR points give little improvement for the estimate for L^{tot}, but impose bounds on A_V.

The predictive potential of two data points in combination with the model library is visualized in Fig. 6 for the ULIRG NGC 6240. It also stresses the relevance of long wavelength observations which radically cut the number of acceptable models and fix the dust mass. The figure also demonstrates the quality of flux extrapolation to wavelengths which have not yet been observed.

5. Discussion

5.1. Methods of modeling starburst SEDs

One finds in the literature three different ways to reproduce or explain the SED of an extragalactic object.

i) Matching it with a template SED of a well known galaxy (Laurent et al. 2000; Chary & Elbaz 2001; Lutz et al. 2003; Spoon et al. 2005). This is reasonable only as long as template and object are similar in their parameters as well as geometrical structure and orientation on the sky: So it is not meaningful to compare SEDs of AGN type 1 and type 2, or objects with radically different luminosities, like M 82 and NGC 6240, because the luminosity affects the SED, as can be seen from Fig. 1a. To obtain a good match between the SED of the object and the template, after normalization to a unit distance, one usually has to scale the flux of the template moderately up or down to fine-tune the luminosity. If the fit is successful one may argue that the object is similar to the template in its geometry and basic parameters (but for some scale factor) and that one understands it almost as well as the template.
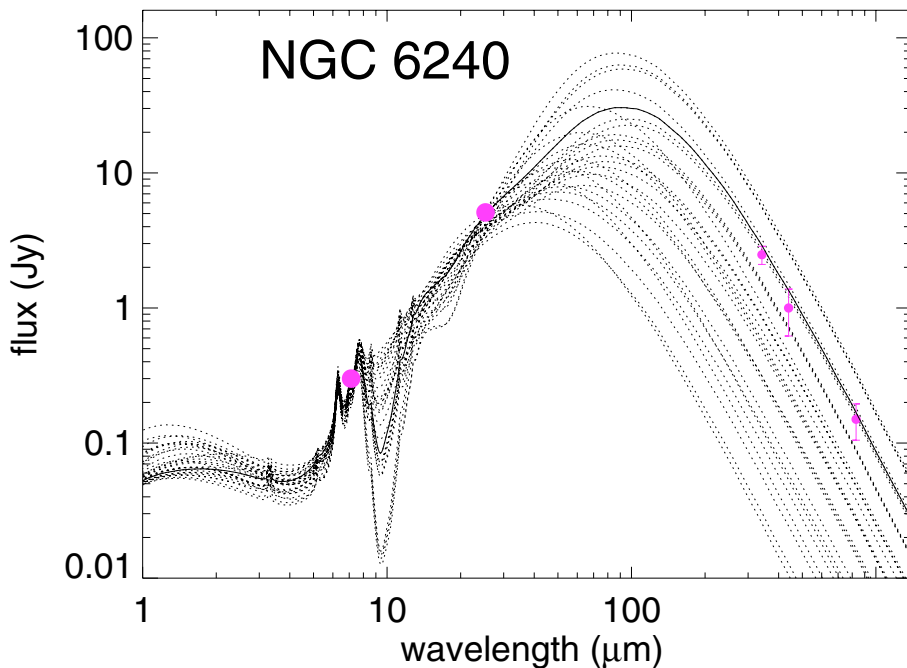
Fig. 6. All elements of the SED library (dotted) which fit 8 and 24 μm photometry (circles) of NGC 6240 to within 30%. Best fit (full line) and other data as of Fig. 5.

ii) Reproducing the shape of the SED by optically thin dust emission. The dust is assumed to be heated in a given radiation field which is usually a scaled-up version of the interstellar field (Devriendt et al. 1999; Dale et al. 2001, 2005; Lagache et al. 2003). This procedure neglects all effects of radiative transfer and must fail when dust self-absorption becomes important, most strikingly in the ~10 μm region as shown in Fig. 1d.

iii) Solving the radiative transfer, in various degree of sophistication. This is a much more ambitious method and requires assumptions about the structure and parameters of the galaxy. Three-dimensional codes have been applied to spirals (Kylafis & Bahcall 1987; Popescu et al. 2000; Tuffs et al. 2004) using ray tracing or Monte Carlo techniques (Bianchi et al. 2000). Rowan-Robinson & Crawford (1989) fit IRAS color diagrams of starbursts using a one-dimensional transfer code.

We also do radiative transfer calculations and it may be instructive to point out technical and conceptual differences between our models and those devised recently by other authors (Efstathiou et al. 2000; Takagi et al. 2003; Dopita et al. 2005; and Piovan et al. 2006), although we admit that we did not always find it easy to pin down exactly which approximations our colleagues used (as they may experience difficulties in identifying our assumptions).

All groups evaluate the emission from a dusty medium of spheroidal shape filled with stars, all seem to use similar optical dust constants, and all incorporate small grains with temperature fluctuations (like PAHs). At first glance, the model results appear to agree, but upon closer inspection one finds that the maximum deviations are considerable (factor 4), whereas the fits from our library to the prototype objects (Figs. 2 to 5) are much smaller (Fig. 7).

The major points where our paper differs concern the treatment of the sources, the interstellar extinction curve, the radiative transfer, and the presence or neglect of hot spots.

a) *Stellar sources.* We do not take into account the time evolution of a stellar population after the burst and the possibility that there may have been several episodes of rapid star formation. Our models are therefore simpler and do not allow to constrain the age of the burst(s). The controversial numbers derived for the stellar populations in M 82 (see above) indicate that this is difficult, anyway.

b) *Extinction curve.* We assume galactic dust and do not consider the possibility that it may be a combination of the species found in the Milky Way, LMC or SMC. Again, here our model is simpler, but as the extinction of the sources is usually large ($A_V > 5$ mag), the exact shape of the reddening curve has little effect on the resulting infrared SED.

c) *Radiative transfer.* As far as we can tell, the interaction between dust and radiation is treated consistently only in Takagi et al. (2003) and the present paper. Other authors introduce basic emission units which they compute separately. Such a unit may be a diffuse gas cloud, or a spherical molecular cloud filled with dust and stars that are either continuously smeared out over the cloud or concentrated in the center. The emission units are then scaled up, or a simplified radiative transfer (with constant source function or no reemission) is applied to match the nucleus under consideration. Naturally, when the optical thickness is not small, models without radiative transfer are at some point faulty, although it is hard to quantify how much the simplifications effect the resulting SED.

d) *Hot spots.* They are a particular feature of our models and inevitably arise when a luminous star is enveloped by a cloud with a density considerably above the mean density of the nucleus. Neglecting hot spots seriously underestimates the MIR emission of the nucleus (see Krügel & Siebenmorgen 1994; or Fig. 1c).

e) *Clumpiness.* As discussed in the model description of M 82, the optical and UV flux is best explained by postulating the interstellar medium to be clumped. Clumping is a natural consequence of supernovae explosions; when the surface filling factor is close to one, it has little effect on the SED at wavelengths greater than a few micron. The models that include stellar evolution (Silva et al.; Efstathiou et al.; Takagi et al.; Dopita et al.; Piovan et al.) introduce as an additional
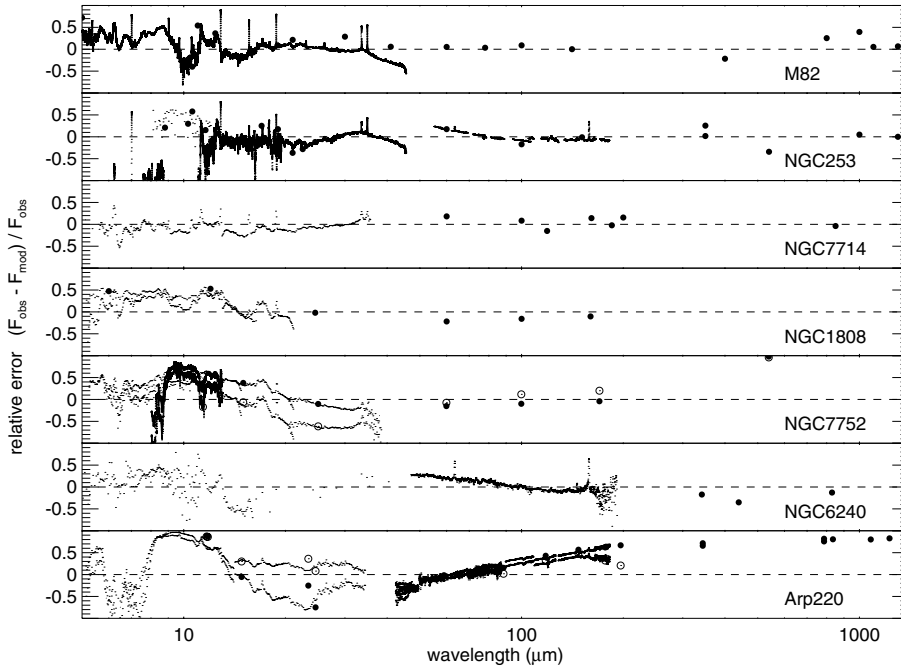
Fig. 7. Relative deviation of model from observations. Broad band data are indicated by filled circles. If there are two models that fit reasonably well, the second is presented by open circles.

free parameter the fraction of starlight escaping the galaxy due to clumping; this fraction depends in their computations on the age of the starburst. Our approach is again simpler. Because the UV and optical stellar light that leaks out is in reality modified in a complicated way by the passage through a clumped medium, we only add, where necessary, a blackbody curve to account for the excess light.

5.2. Completeness, uniqueness and credibility of the SED library

It is remarkable that one can very well fit the SEDs of galaxies, like M 82, Arp 220 and others, with models of constant density and radial symmetry. The satisfactory fits imply, first, that our library grid is sufficiently fine, and we expect that starbursts observed with similar wavelength coverage as those presented in Figs. 2–5 (more than a few data points in the SED) can be reasonably matched by a single element of the SED library.

Nevertheless, one may wonder whether the fits are meaningful. After all, we know for AGN, which have tori that lead to the division into type 1 and 2 with respect to the observer, that spherical symmetry is a principally unacceptable approximation. As the torus is the result of rotation, it should form independently of a massive black hole and therefore also exist in starbursts. However, there seems to be no need to invoke one. There are probably two explanations. First, whereas an AGN is small (pc) and easily shadowed by the much bigger torus (100 pc), a starburst region is as large as or larger than a torus and could not be blocked visually. So there cannot be starbursts of type 1 and 2. Second, the galaxy collision preceding the starburst leads to strong perturbations of the nuclear gas which, in the gravitational potential of the little disturbed bulge stars, results in rough spherical symmetry.

We also have to discuss the possible contamination of starburst fluxes by emission from the galactic disk when the spatial resolution of the observations is poor. This is the standard situation in the far infrared. However, as a starburst nucleus is usually much brighter than the disk, the contamination is irrelevant.

It may be substantial at short wavelengths (NIR, optical, UV) if the starburst is very obscured and little optical flux leaks out.

In the submm/mm region, one measures mainly the dust mass and there is likely to be more mass in the disk than in the core. To estimate the contributions of the disk and the core, let F, L, M and T denote the observed flux, bolometric luminosity, dust mass and dust temperature, respectively. With the approximations $L \propto MT^6$ and $F_{1\,mm} \propto MB_{1\,mm}(T) \propto MT$, the flux ratio at 1 mm, becomes $F_{1\,mm,c}/F_{1\,mm,d} = (L_c/L_d)(T_d/T_c)^5$. Here we used the index d for disk and c for the core. Typical mean values are $T_d = 10\ldots20$ K (Krügel et al. 1998) and $T_c = 30\ldots50$ K (Klaas et al. 2001). Therefore, the cold dust in the disk is not really important in measurements of low spatial resolution as long as the nucleus is much brighter than the disk.

5.3. Application to high redshift galaxies

The library also seems to be applicable to extremely luminous objects at large redshifts. We demonstrate this in Fig. 8 for the submillimeter galaxy MMJ154127+6616 which is at $z = 2.8$ as derived from the identification of PAH features in the Spitzer IRS low resolution spectrum (Lutz et al. 2005). MMJ154127+6616 seems to be an extremely massive object (10^{11} $M_\odot$) where the starburst comprises the whole galaxy.

For luminosities above $10^{12.7}$ $L_\odot$ and radii ≥ 9 kpc, we have therefore modified the structure of the models accordingly. *a)* The size is increased to $R = 9$ kpc and 15 kpc. *b)* There are only OB stars as giants have had no time to evolve. 40% of the stars are assumed to be in regions of enhaned density (hot spots). *c)* The star formation region extends to the edge of the galaxy.

One finds two entries in the library which are compatible with the observations (Fig. 8), both imply extreme luminosities ($L_{dust} = 10^{13.7}$ $L_\odot$) and dust masses close to 10^{10} $M_\odot$.

6. Conclusions

We have computed in a self-consistent radiative transfer SEDs of spherical, dusty galactic nuclei over a wide range of their basic

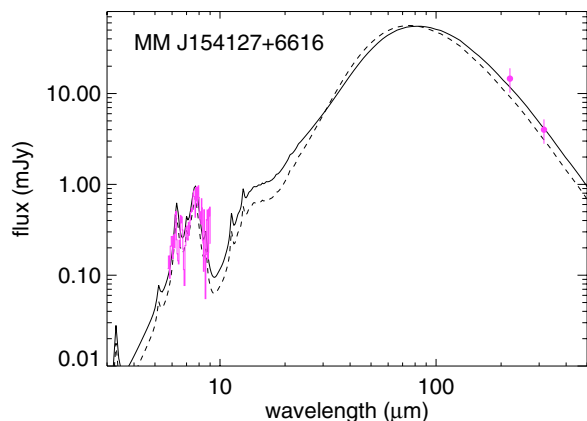**Fig. 8.** The spectrum of MMJ154127+6616 in the restframe of the galaxy ($z = 2.8$) with two library models. Model parameters: *solid line:* $L = 10^{13.7} L_{\odot}$, $A_V = 70$ mag, $R = 15$ kpc; *dashed line:* $L = 10^{13.7} L_{\odot}$, $A_V = 120$ mag, $R = 9$ kpc. Observational points from Lutz et al. (2005), Eales et al. (2003) and Bertoldi et al. (2000).

parameters such as luminosity, dust mass, size and obscuration. The SEDs can be accessed in a public library[1].

Given a set of data points for a particular galaxy, there is a simple procedure, described in the README file, to select from the library those elements which best match them. If the observations cover the full wavelengths band from a few μm to about 1 mm, one usually finds only one library element that fits very well, as demonstrated for seven famous active galaxies. If the data points are widely spaced, there may be a few elements of less fitting quality, but similar in their basic parameters.

The library therefore allows one to constrain the fundamental properties of any nucleus which is powered by star formation and for which data exist, without any further modeling. Two observed fluxes in the MIR plus one submm point are usually sufficient for a crude characterization of the nucleus. If there are only two MIR points, for example, from Spitzer at 8 and 24 μm, one can still bracket the total luminosity within a factor of ~2.

In the UV, optical and NIR, it may be necessary to add to the library SED a low luminosity stellar component, at least, this was necessary for M 82 and NGC 6240. This component may be due to photons that escaped the nucleus without interaction because of clumping or it may be light from the galactic disk.

References

Aaronson, M. 1977, Ph.D. Thesis Harvard Univ., Cambridge, MA
Benford, D. J. 1999, Ph.D. Thesis, California Institute of Technology (USA)
Bertoldi, F., Carilli, C. L., Menten, K. M., et al. 2000, A&A, 360, 92
Bianchi, S., Davies, J. I., & Alton, P. B. 2000, A&A, 359, 65
Brandl, B. R., Devost, D., Higdon, S. J. U., et al. 2004, ApJ, 154, 184
Carico, D. P., Keene, J., Soifer, B. T., & Neugebauer, G. 1992, PASP104, 681
Chary, R., & Elbaz, D. 2001, ApJ, 556, 562

Chini, R., Kreysa, E., Mezger, P. G., & Gemuend, H.-P. 1984, A&A, 137, 117
Chini, R., Kreysa, E., Krügel, E., & Mezger, P. G. 1986, A&A, 166, 8
Dale, D. A., Helou, G., Contursi, A., Silbermann, N. A., & Kolhatkar, S. 2001, ApJ, 549, 215
Dale, D. A., Bendo, G. J., Engelbracht, C. W., et al. 2005, ApJ, 633, 857
Devriendt, J. E., Guiderdoni, B., & Sadat, R. 1999, A&A, 350, 381
Dopita, M. A., Groves, B. A., Fishcera, J., et al. 2005, ApJ, 619, 755
Dunne, L., Eales, S., Edmunds, M., et al. 2000, MNRAS, 315, 115
Eales, S., Bertoldi, F., Ivison, R., et al. 2003, MNRAS, 344, 169
Efstathiou, A., & Siebenmorgen, R. 2005, A&A, 439, 85
Efstathiou, A., Rowan-Robinson, M., & Siebenmorgen, R. 2000, MNRAS, 313, 734
Floc'h, E., Papovich, C., Dole, H., et al. 2005, ApJ, 632, 169
Galliano, E., Alloin, D., Pantin, E., Lagage, P. O., & Marco, O. 2005, A&A, 438, 803
Glass, I. S. 1976, MNRAS, 175, 191
Guhathakurta, P., & Draine, B. T. 1989, ApJ, 345, 230
Heckman, T. M., Armus, L., & Miley, G. K. 1990, ApJS, 74, 833
Heckman, T. M. 1998, ASP Conf. Ser., 148, 127
Higdon, S. J. U., Devost, D., Higdon, J. L., et al. 2004, PASP, 116, 975
Hildebrand, R. H., Whitcomb, S. E., Winston, R., et al. 1977, ApJ, 216, 698
Hirashita, H., Buat, V., & Inoue, A. K. 2003, A&A, 410, 83
Hughes, D. H., Gear, W. K., & Robson, E. I. 1990, MNRAS, 244, 759
Imanishi, M., & Maloney, P. 2003, ApJ, 588, 165
Jaffe, D. T., Becklin, E. E., & Hildebrand, R. H. 1984, ApJ, 285, L31
Jarrett, T. H., Chester, T., Cutri, R., Schneider, S. E., & Huchra, J. P. 2003, AJ, 125, 525
Johnson, H. L. 1966, ApJ, 143, 187
Kennicutt, R. C., Jr., Keel, W. C., van der Hulst, J. M., Hummel, E., & Roettiger, K. A. 1987, AJ, 93, 1011
Kennicutt, R. C., Jr., Armus, L., Bendo, G., et al. 2003, PASP, 115, 928
Klaas, U., Haas, M., Heinrichsen, I., & Schulz, B. 1997, A&A, 325, L21
Klaas, U., Haas, M., Müller, S. A. H., et al. 2001, A&A, 379, 823
Kleinmann, D. E., & Low, F. J. 1970, ApJ, 159, L165
Krabbe, P. P., Steinberg, A., & Genzel, R. 1994, ApJ, 425, 72
Krügel, E. 2003, The physics of interstellar dust (IOP Publishing Ltd.)
Krügel, E., & Siebenmorgen, R. 1994, A&A, 282, 407
Krügel, E., & Tutokov, A. V. 1978, A&A, 63, 375
Krügel, E., Chini, R., Klein, U., et al. 1990, A&A, 240, 232
Krügel, E., Siebenmorgen, R., Zota, V., & Chini, R. 1998, A&A, 331, L9
Kylafis, N. D., & Bahcall, J. N. 1987, ApJ, 317, 637
Laurent, O., Mirabel, I. F., Charmandaris, V., et al. 2000, A&A, 359, 887
Lutz, D., Sturm, E., Genzel, R., et al. 2003, A&A, 409, 867
Lutz, D., Valiante, E., Sturm, E., et al. 2005, ApJ, 625, L83
Piovan, L., Tantalo, R., & Chiosi, C. 2006, MNRAS, 366, 923
Popescu, C. C., Misiriotis, A., Kylafis, N. D., et al. 2000, A&A, 362, 138
Radovich, M., Kahanpää, J., & Lemke, D. 2001, A&A, 377, 73
Rieke, G. H., & Low, F. J. 1972, ApJ, 176, L95
Rieke, G. H., & Low, F. J. 1975, ApJ, 197, 17
Rieke, G. H., Harper, D. A., Low, F. J., & Armstrong, K. R. 1973, ApJ, 183, 67
Rieke, G. H., Lebofsky, M. J., Thompson, R. I., et al. 1980, ApJ, 328, 24
Roussel, H., Vigroux, L., & Bosma, A. 2001, A&A, 369, 473
Rowan-Robinson, M., & Crwaford, J. 1989, MNRAS, 238, 523
Siebenmorgen, R., Krügel, E., & Zota, V. 1999, A&A, 351, 140
Siebenmorgen, R., & Efstathiou, A. 2001, A&A, 376, L35
Siebenmorgen, R., Krügel, E., & Laureijs, R. J. 2001, A&A, 377, 735
Siebenmorgen, R., Krügel, E., & Spoon, H. W. W. 2004, A&A, 414, 123
Silva, L., Granato, G. L., & Bressan, A. 1998, ApJ, 506, 600
Sloan, G. C., Kraemer, K. E., Price, S. D., & Shipman, R. F. 2003, ApJS, 147, 379
Spinoglio, L., Malkan, M. A., Rush, B., Carrasco, L., & Recillas-Cruz, E. 1995, ApJ, 453, 616
Spoon, H. W. W., Moorwood, A. F. M., Lutz, D., et al. 2004, A&A, 414, 873
Spoon, H. W. W., Keane, J. V., Cami, J., et al. 2005, IAU Symp., 231, 281
Stickel, M., Lemke, D., Klaas, U., & Krause, O. 2004, A&A, 422, 39
Takagi, T., Arimoto, N., & Hanami, H. 2003, MNRAS, 340, 813
Takeuchi, T. T., Ishii, T. T., Dole, H., et al. 2006, A&A, 448, 525
Telesco, C. M., & Harper 1980, ApJ, 235, 392
Telesco, C. M., & Gezari, D. Y. 1992, ApJ, 395, 461
Tuffs, R., Popescu, C. C., Völk, H. J., et al. 2004, A&A, 419, 821

[1] The SED library is available at:
http://www.eso.org/~rsiebenm/sb_models